Program Digest, 2019 IEEE International Ultrasonics Symposium (IUS)
Glasgow, Scotland, October 6-9, 2019

High contrast imaging of low boiling point phase change contrast agents in moving tissue with ultrafast inter-frame activation imaging sequence

Bowen Jing
Coulter Department of Biomedical Engineering, Georgia Institute of Technology and Emory University, Atlanta, Georgia, USA
bowen.jing@bme.gatech.edu

Milton E. Brown
Division of Cardiology, Department of Medicine, Emory University, Atlanta, Georgia, USA
mebrow5@emory.edu

Michael E. Davis
Coulter Department of Biomedical Engineering, Georgia Institute of Technology and Emory University, Atlanta, Georgia, USA
michael.davis@bme.gatech.edu

Brooks D. Lindsey
Coulter Department of Biomedical Engineering, Georgia Institute of Technology and Emory University, Atlanta, Georgia, USA
brooks.lindsey@bme.gatech.edu

***Abstract*— Nanoscale phase change contrast agents (PCCA) have been demonstrated for extravascular imaging in tissue. However, contrast in PCCA images is typically limited by physiological motion and incomplete cancelation of unwanted tissue signal. In this work, we develop an ultrafast inter-frame activation imaging sequence for high contrast PCCA imaging in the presence of physiological motion by imaging the inter-frame variation produced by activation of PCCA, which is distinguishable from tissue and blood motion. Phantom studies indicate that in the absence of tissue motion, the CTR of UIAU images is 19.55±0.42 dB while the CTR of the amplitude modulate + pulse inversion (AMPI) is 8.15±0.65 dB and the CTR of differential imaging is 24.20±1.22 dB. Furthermore, the CTR of these UIAU images can reach 51.43±3.3 dB by applying a denoising approach. With 20 mm/s motion, the CTR of UIAU and denoised UIAU images were 18.70±1.40 dB and 31.77±9.76 dB respectively, which were both significantly higher than that of amplitude modulation + pulse inversion (AMPI) and differential images. The preliminary *in vivo* imaging results indicate the UIAU could significantly suppress the background tissue in the presence of physiological motion.**

Keywords*— *Contrast-to-tissue ratio, nanoscale phase change contrast agents, ultrafast inter-frame activation ultrasound

I. Introduction

The nanoscale phase change contrast agent (PCCA), which is comprised of deformable shell and volatile perfluorocarbon core, can be vaporized from liquid nanodroplets to gaseous bubbles by applying laser or ultrasound pulses [1, 2]. This process is also referred to as activation of PCCAs. The PCCA nanodroplet is hypoechoic in ultrasound images, while the gas bubble is an echogenic, bright contrast agent in the image. Due to the longer circulation lifetime and nanoscale diameter, the PCCA has potential advantages for extravascular, molecular imaging [3] and image-guided therapeutic applications [4].

Because PCCAs vaporize into microbubbles, conventional contrast-specific imaging techniques have been used for PCCA imaging. These include pulse inversion [5] and amplitude modulation + pulse inversion approaches [6], both of which utilize the nonlinear acoustic response of the microbubble. In order to further suppress the tissue signal and improve the contrast, differential imaging has also been used [7]. Differential images are obtained by subtracting the baseline image from the post-activation image in order to remove the tissue signal. However, the physiological tissue motion can significantly degrade the performance of this method. Another imaging approach has also been proposed recently to acquire the image of PCCAs by detecting the low frequency oscillation of PCCAs when they vaporize [8]. However, the spatial resolution of this approach is much lower than other techniques.

In the present study, an ultrafast inter-frame activation ultrasound (UIAU) imaging approach is proposed and evaluated. Steerable focused ultrasound beams are used to activate the PCCAs in the region of interest (ROI). High frame rate ultrasound imaging events are interleaved with the focused activation beams to record the activation of PCCAs. The high frequency fluctuation of the PCCA signal over subsequent acquisitions is then separated from the low frequency signal of moving tissues by using a high pass clutter filter. A similar imaging approach for interleaving the activation and imaging events was proposed for super-resolution imaging [9]. However, it should be noted that the imaging frame rate of our proposed approach is 2000 fps which is much higher than 100 fps in the previous study, in order to enable image-guided delivery even in the presence of significant physiological motion (e.g. respiratory or cardiac). The first advantage of the high frame rate is the temporal resolution. Given an ensemble length of 100 to 200 frames, the final imaging temporal resolution would be below

This work was supported in part by the Department of Biomedical Engineering and the College of Engineering at Georgia Institute of Technology and by R01HL144714 from the National Institutes of Health.

0.1 second. Furthermore, the 2000 fps sampling rate also enables the application of a high pass filter to separate the PCCA signal from tissue signals, including the microvascular signal in the frequency domain, which would be challenging to achieve using singular value decomposition filtering. This approach could be useful for identifying the local aggregation of PCCAs in extravascular space (e.g. in tumors or regions of infarct).

II. Materials and Methods

A. Ultrasound imaging sequence:

For the UIAU imaging sequence, 3 steered (-10°, 0° and 10°), unfocused beams were sequentially transmitted at a pulse repetition frequency of 10 kHz to insonify the region of interest. Single-cycle 5 MHz pulses were used to generate a free field peak negative pressure of 370 kPa at a depth of 10 mm. For each transmit event, the echo was received, beamformed and demodulated to produce a set of in-phase/quadrature (IQ) data. The transmitting of 3 steered imaging beam was repeated at 200 times at 2000 Hz. Following each packet of 3 unfocused beams, focused beams of 3-cycle 5 MHz pulses were transmitted to activate PCCAs. The derated (0.5 dB/[cm·MHz]) peak negative pressure is 3.52 MPa at a depth of 10 mm. The beam focus was being steered and shifted during imaging to activate PCCAs across the region of interest.

3 sets of IQ data were acquired at 3 transmitting angles. The IQ data were filtered in slow time at each pixel using an 8^{th}-order high pass filter to suppress low frequency tissue signal. Then, the IQ data from the -10° and 10° transmits were summed coherently. The cross correlation between the 0° IQ data and the previously summed IQ data was calculated at each pixel. The UIAU image was obtained by taking the square root of the real part of the correlation value.

In addition, based on the UIAU acquisitions and clutter filtering, the UIAU image was further denoised by subtracting the noise floor from the autocorrelation estimation of signal power [10]. The autocorrelation estimation was obtained by coherently summing the 3 sets of IQ data (-10°, 0° and 10°) and taking the zero-lag autocorrelation at each pixel. The noise floor is obtained in the same way as the autocorrelation, however with the transmitters of the scanner disabled to acquire random noise. Since the signal power should be non-negative, the negative pixels were all set zero. The final denoised UIAU image was the square root of the estimated signal power at each pixel.

The UIAU was also compared with the amplitude modulation + pulse inversion (AMPI) and the differential imaging approaches in the present study. Unfocused wave transmit events were used for the amplitude modulation + pulse inversion approach [11]. 17 steered transmit events at varying angles (-10° to 10°) were used. The total number of transmit events was 51 (3 pulses per angle): 1 full-amplitude pulse and 2 inverted half-amplitude pulses. The differential images were obtained by subtracting the pre-activation frame of AMPI from the corresponding post-activation frame. Between the pre-activation and post-activation frame, steered and focused activation beams were used to activate the PCCAs across the same ROI as that in UIAU sequence. The interval between the pre-activation and post-activation acquisitions was 20 ms.

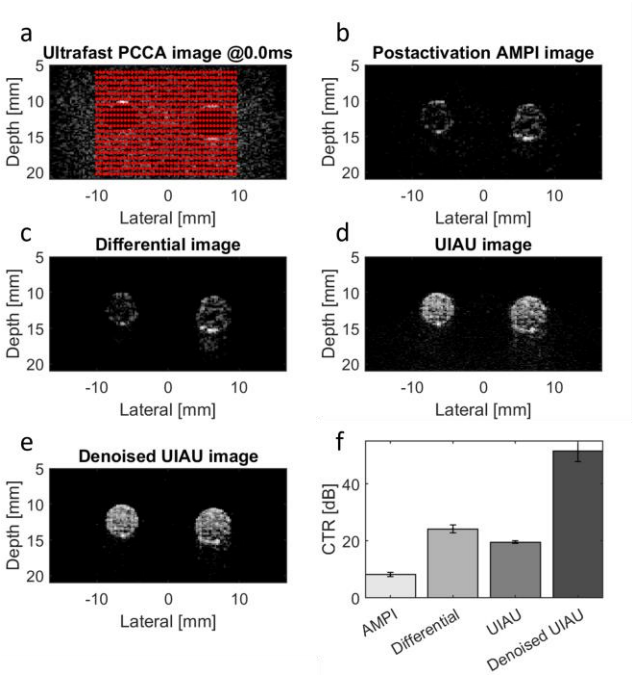

Fig.1. Images of PCCAs in the phantom channels. (a) The activation beam foci overlaid on pre-activation B mode image. (b) The amplitude modulated pulse inversion image of the vaporized PCCAs. (c) The differential image of PCCAs. (d) The UIAU image. (e) The denoised UIAU image. (f) The contrast-to-tissue ratio of different imaging approaches.

B. Phantom study:

A gelatin phantom with 2 parallel 10 mm deep channels was fabricated and used. Graphite powder (0.06 g/ml) was added into the phantom. The attenuation was estimated to be ~0.5 dB/[cm·MHz]. Decafluorobutane (DFB) nanodroplets [2] were diluted by a factor of 400 in degassed water at 35 C° to 37 C°. According to the measurements obtained using a NanoSight NS300 (Malvern Instruments, Westborough, MA, USA), the concentration of the nanodroplets solution was 10^8 particles/ml. The images of the phantom was acquired using UIAU, AMPI and differential imaging approaches.

After the images of the phantom were acquired without motion, 20 mm/s of motion along the axial direction was introduced using a motion stage (XPS-Q8, Newport, Irvine, CA, USA) and the images were acquired. A 128-element linear array transducer (L11-5, ATL, Bothell, WA, USA) connected to an ultrasound scanner (Vantage 256, Verasonics, Kirkland, WA, USA) was used.

The contrast-to-tissue ratio (CTR), i.e. $CTR = 20\times log_{10}(S_{PCCA}/S_{Tissue})$, was obtained. S_{PCCA} is the mean PCCA signal magnitude and S_{Tissue} is mean tissue signal magnitude.

C. In vivo study:

A 5-6 week-old male Sprague-Dawley rat (Envigo, Greenfield, IN, USA) was imaged to demonstrate the performance of UIAU in vivo. The L11-5 array was used. The animal study protocol was approved by the Institutional Animal Care and Use Committee of Emory University. The images of the liver were acquired. Instead of using AMPI, full amplitude pulse inversion approach was used in this part of study. During

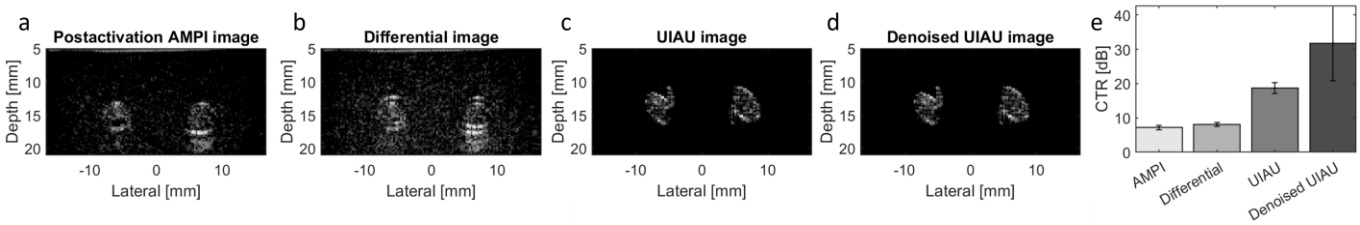

Fig. 2. Images of PCCAs in phantom channel with 20 mm/s motion along the beam axial diretion. (a) AMPI image. (b) Differential image. (c) UIAU image. (d) Denoised UIAU image. (e) The contrast-to-tissue ratio of different imaging approaches.

the experiment, the rats were anesthetized using 2.5% isoflurane. Before injection, the DFB nanodroplets were diluted by a factor of 2 (~10^{10} particles/ml). 0.1 ml of nanodroplets solution was injected for a 150 g rat through the tail vein.

III. Results

A. Phantom study:

A 15×20 mm^2 rectangular region was scanned using the steered, focused activation beams as indicated by the red foci in Fig. 1a. The channels became echogenic after the vaporization of the PCCAs, as shown in the AMPI image (Fig. 1b). Similar echogenic patterns were seen in the differential image (Fig. 1c). With the proposed UIAU approach, the channels appeared hyperechoic relative to the hypoechoic tissue background (Fig. 1d and Fig. 1e). The contrast-to-tissue ratios of UIAU and denoised UIAU images were significantly ($p < 0.01$) higher than AMPI images (Fig. 1f), while differential image was significantly ($p < 0.01$) higher than UIAU image for the stationary case. The denoised UIAU image provided the highest CTR among all approaches.

When 20 mm/s motion was introduced along the beam in the axial direction, the tissue background became significantly brighter in the differential image (Fig. 2b) compared to the case without motion. Due to the high motion, the channels in the UIAU images (Fig. 2c and d) appear distorted since the UIAU images were actually obtained by compounding the whole ensemble of 200 frames lasting 0.1 second. Motion correction approaches could be potentially used to correct the distortion. Despite this, CTR of UIAU images was significantly higher than that of AMPI and differential images, as shown in Fig. 2e.

B. In vivo study:

The activated PCCAs appeared as a matrix of echogenic points in the liver tissue below the skin surface (Fig. 3a). The skin was visible in both pulse inversion and differential images (Fig. 3b). Alternatively, the tissue including the skin was not visible in the UIAU images (Fig. 3c and d). Moreover, the noisy deep part (≥20 mm) of the UIAU image (Fig. 3c) was removed by denoising (Fig. 3d). All the images in Fig. 3 are shown with 30 dB dynamic range.

IV. Conclusion

An ultrafast inter-frame activation ultrasound imaging sequence was proposed to activate phase change nanodroplets and improve the contrast-to-tissue ratio in the presence of physiological motion. The phantom imaging results indicated UIAU provided significantly higher CTR than the amplitude modulation + pulse inversion approach. Due to the high-pass

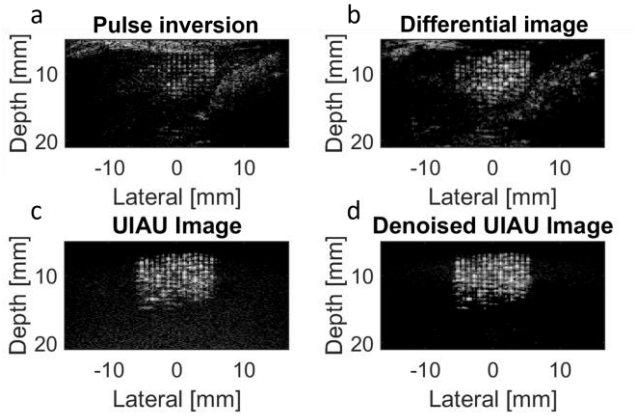

Fig.3. Images of PCCAs in the rat liver: (a) Pulse inversion image, (b) Differential image, (c) UIAU image, and (d) denoised UIAU image.

clutter filtering strategy, the UIAU approach was more robust to tissue motion than differential imaging. In addition, a denoising strategy further improved the CTR of UIAU image. Overall, the UIAU technique is a promising imaging tool for locally activating and visualizing extravascular, nanoscale PCCAs in the presence of significant physiological motion. This technique can potentially be used for PCCA-based extravascular imaging, targeted molecular imaging, and image-guided drug delivery, all of which require imaging low concentrations of PCCAs.

Acknowledgment

The authors thank Graham Collins and Yutong Guo for assistance with experimental preparation and thank Jesutoyosi Awoyeye for assistance with synthesizing contrast agents. This work was supported in part by the Department of Biomedical Engineering and the College of Engineering at Georgia Institute of Technology and by R01HL144714 from the National Institutes of Health.

References

[1] A. S. Hannah, G. P. Luke, and S. Y. Emelianov, "Blinking phase-change nanocapsules enable background-free ultrasound imaging," Theranostics, vol. 6, no. 11, pp. 1866-1876, 2016.

[2] P. S. Sheeran et al., "Decafluorobutane as a phase-change contrast agent for low-energy extravascular ultrasonic imaging," Ultrasound in Medicine and Biology, vol. 37, no. 9, pp. 1518-1530, Sep 2011.

[3] R. Williams et al., "Characterization of submicron phase-change perfluorocarbon droplets for extravascular ultrasound imaging of cancer," Ultrasound in Medicine and Biology, vol. 39, no. 3, pp. 475-489, Mar 2013.

[4] S. M. Fix et al., "Ultrasound-stimulated phase-change contrast agents for transepithelial delivery of macromolecules, toward gastrointestinal drug delivery," Ultrasound in Medicine and Biology, vol. 45, no. 7, pp. 1762-1776, 2019.

[5] P. S. Sheeran, J. D. Rojas, C. Puett, J. Hjelmquist, C. B. Arena, and P. A. Dayton, "Contrast-enhanced ultrasound imaging and in vivo circulatory kinetics with low-boiling-point nanoscale phase-change perfluorocarbon agents," Ultrasound in Medicine and Biology, vol. 41, no. 3, pp. 814-831, 2015.

[6] J. D. Rojas and P. A. Dayton, "In vivo molecular imaging using low-boiling-point phase-change contrast agents: a proof of concept study," Ultrasound in Medicine and Biology, vol. 45, no. 1, pp. 177-191, 2019.

[7] H. Yoon and S. Y. Emelianov, "Combined multiwavelength photoacoustic and plane-wave ultrasound imaging for probing dynamic phase-change contrast agents," IEEE Transactions on Biomedical Engineering, vol. 66, no. 2, pp. 595-598, 2018.

[8] J. D. Rojas and P. A. Dayton, "Vaporization detection imaging: a technique for imaging low-boiling-point phase-change contrast agents with a high depth of penetration and contrast-to-tissue ratio," Ultrasound in Medicine and Biology, vol. 45, no. 1, pp. 192-207, 2019.

[9] G. Zhang et al., "Acoustic wave sparsely activated localization microscopy (AWSALM): Super-resolution ultrasound imaging using acoustic activation and deactivation of nanodroplets," Applied Physics Letters, vol. 113, no. 1, p. 014101, Jul 2 2018.

[10] C. Huang, P. Song, P. Gong, J. D. Trzasko, A. Manduca, and S. Chen, "Debiasing-based noise suppression for ultrafast ultrasound microvessel imaging," IEEE Transactions on Ultrasonics, Ferroelectrics, and Frequency Control, vol. 66, no. 8, pp. 1281-1291, 2019.

[11] O. Couture, M. Fink, and M. Tanter, "Ultrasound contrast plane wave imaging," IEEE Transactions on Ultrasonics, Ferroelectrics, and Frequency Control, vol. 59, no. 12, pp. 2676-2683, 2012.